Low-temperature heat capacity of magnetic graphite intercalation compounds

M. Shayegan* and M. S. Dresselhaus
Department of Electrical Engineering and Computer Science and Center for Materials Science and Engineering, Massachusetts Institute of Technology, Cambridge, Massachusetts 02139

L. Salamanca-Riba
Department of Physics and Center for Materials Science and Engineering, Massachusetts Institute of Technology, Cambridge, Massachusetts 02139

G. Dresselhaus
Francis Bitter National Magnet Laboratory, Massachusetts Institute of Technology, Cambridge, Massachusetts 02139

J. Heremans and J.-P. Issi
Laboratoire de Physico-Chimie et de Physique de l'État Solide, Place Croix du Sud, 1 B-1348 Louvain-la-Neuve, Belgium

(Received 4 April 1983)

The heat capacity C_p of magnetic graphite intercalation compounds $C_{\xi n}(CoCl_2)_{1-q}(AlCl_3)_q$ (stages $n=2,4,5$) is measured as a function of temperature ($3<T<25$ K) at zero and high (up to 14 T) magnetic fields ($\vec{H}$ applied in plane). We are able to separate C_p into its electronic, lattice, and magnetic contributions by suppressing the magnetic contribution to C_p at the highest magnetic fields. The electronic heat capacity C_E is observed to be small (for $T>3$ K) compared with the lattice contribution C_L which exhibits a T^2 temperature dependence characteristic of a two-dimensional phonon spectrum. The small value of C_E is consistent with the results of our Fermi-surface measurements, which show excellent agreement with the predictions of the rigid-band model and c-axis zone folding. The magnetic heat capacity C_M shows a broad peak at $\simeq 9.1$ K. The shape of this peak is consistent with the reported Monte Carlo calculations of C_M based on a two-dimensional XY model.

I. INTRODUCTION

The magnetic graphite intercalation compounds (GIC), formed by the insertion of magnetic intercalants (e.g., $FeCl_3$, $CoCl_2$, and $NiCl_2$) between the graphite layers, provide a system in which the layers of the magnetic material can be separated by a controlled number (equal to stage n) of graphite layers which are diamagnetic in pristine graphite. Previous studies[1-7] of the temperature dependence of the magnetic susceptibility $\chi(T)$ and heat capacity at constant pressure $C_p(T)$ have shown that these compounds undergo magnetic phase transitions at low temperatures. Although the nature of this magnetic ordering is not fully understood yet, the experimental results have established that the magnetic ordering temperatures in these GIC are nearly stage independent and that they are lower than those of the parent (intercalant) material. These magnetic states have thus been attributed to two-dimensional magnetic interactions in the GIC. In view of recent theoretical interest in the study of phase transitions in two-dimensional (2D) systems, the magnetic GIC have become the subject of renewed attention.

As a result of the pioneering measurements of $\chi(T)$ for $NiCl_2$-GIC, $CoCl_2$-GIC, and $FeCl_3$-GIC by Karimov *et al.*[1,2] and some recent studies,[3-7] it has been inferred that at least in some temperature range $T_{c1}\leq T\leq T_{c2}$ an intermediate 2D XY-like[8,9] phase exists for these compounds. Below T_{c1}, a symmetry-breaking field with sixfold symmetry due to the intercalate layer has a large effect, giving rise to a transition to a magnetic state with a net magnetization.[3,9] In reported studies of $\chi(T)$ for magnetic GIC, the functional form of $\chi(T)$ has been interpreted in terms of the two-dimensional XY model.[3,6] Considering the nature of the magnetic structure of the parent (intercalant) material (e.g., pristine $CoCl_2$), this reported 2D behavior for the intercalation compounds (e.g., $CoCl_2$-GIC) is not surprising. Pristine $CoCl_2$ undergoes an antiferromagnetic phase transition at the Néel temperature $T_N=24.9$ K, below which the spins are aligned in 2D ferromagnetic sheets which are stacked antiferromagnetically.[10,11] The magnetic Hamiltonian for $CoCl_2$ can be written as

$$H=-J\sum_{\langle ij\rangle}\vec{S}_i\cdot\vec{S}_j+J_A\sum_{\langle ij\rangle}S_i^zS_j^z-J'\sum_{\langle ik\rangle}\vec{S}_i\cdot\vec{S}_k$$
$$+J_A'\sum_{\langle ik\rangle}S_i^zS_k^z\ , \qquad (1)$$

where the sums are over spin pairs and the exchange constants deduced from neutron scattering experiments[11] are reported to be $J=(28.5\ \text{K})k_B$ and $J'=(2.2\ \text{K})k_B$ for the intraplanar and interplanar interactions, respectively, indi-

cating an anisotropy factor of $J/J' \simeq 13$. (Here k_B is the Boltzmann constant.) In the Hamiltonian of Eq. (1), J_A and J'_A are the exchange constants, representing XY-type interactions, and have values $J_A = (16.0\ \text{K})k_B$ and $J'_A = (3.3\ \text{K})k_B$, respectively.[11] The anisotropy J/J' is expected to be even larger for the graphite-$CoCl_2$ compounds because of the presence of the diamagnetic graphite planes between adjacent $CoCl_2$ layers. In fact, from the field-dependent behavior of the $\chi(T)$ measurements on a stage-2 $CoCl_2$-$AlCl_3$-GIC in our laboratory, J/J' is inferred to be larger than 5000 in $CoCl_2$-$AlCl_3$-GIC.[12,13] Thus quasi-2D behavior of the magnetic phases for magnetic GIC (such as $CoCl_2$-GIC) is expected.

In the present work we have made measurements of the heat capacity $C_p(T)$ for the graphite-$CoCl_2$ compounds, in order to further characterize the phase transitions in magnetic GIC and also to learn about their electronic and lattice properties. For a magnetic compound, $C_p(T)$ is usually written as

$$C_p(T) = C_E(T) + C_L(T) + C_M(T)\ , \tag{2}$$

where C_E, C_L, and C_M are the electronic, lattice, and magnetic contributions to C_p, respectively. The goal of this study is to separate $C_p(T)$ in Eq. (2) into its three components and to understand each of these contributions. The temperature dependence of the heat capacities of graphite intercalated with $NiCl_2$ (Refs. 1 and 5), $CoCl_2$ (Ref. 2), and $FeCl_3$ (Ref. 5) have been previously reported. In most of these studies, $C_p(T)$ was measured in zero applied magnetic field, and the method of corresponding states[14] was used to separate C_M from $C_E + C_L$. In the method of corresponding states, C_M for a magnetic compound (e.g., $CoCl_2$) is estimated by subtracting the C_p of a nonmagnetic compound with similar structure (such as $MnCl_2$ which is nonmagnetic in the temperature range where the subtraction is made) from C_p for the magnetic compound.[10]

The assumption of the method of corresponding states is that the $C_L + C_E$ contributions to C_p for the two compounds are the same. In determining C_M for a magnetic GIC, however, one should be cautious about using this method because it is rather difficult to grow two GIC samples with identical structures. The presence of secondary (admixed) stages, differences in in-plane densities, and the presence of intercalate islands and vacancies are among the considerations encountered in attempting to grow GIC with identical structures. In our study, therefore, we employed another method to provide a more definitive measurement of C_M; this method used the same sample without invoking measurements of C_p for other compounds.

Our method consists of measuring C_p as a function of temperature at zero magnetic field and at high applied fields (up to 14 T). If the magnetic field (applied in the plane of the intercalant) is sufficiently large so that we are in the spin-aligned paramagnetic state, there will be no magnetic contribution to C_p, thus permitting us to find C_M as the difference between the zero- and high-field C_p. We can then compare our C_M data with recent Monte Carlo calculations for C_M based on the XY model.[15]

In this study, we selected the $CoCl_2$-GIC system as a prototype magnetic system for the following reasons. Its magnetic transition temperature $T_c \simeq 9$ K is in a range which is easily attainable experimentally and the saturating magnetic field estimated by $H' = k_B T_c / \mu_B \simeq 13$ T (where μ_B is the Bohr magneton) is also in an experimentally available range. Also, the XY anisotropy factor $J_A/J \cong 0.56$ [see Eq. (1)] for pristine $CoCl_2$ is the largest among the known magnetic intercalants for GIC.

II. EXPERIMENTAL DETAILS

The intercalated graphite samples were prepared from highly oriented pyrolytic graphite (HOPG) using the two-zone technique.[16] The HOPG crystals of in-plane dimensions $\sim 4 \times 15$ mm^2 and thicknesses between 0.1 and 0.5 mm were placed at one end of a Pyrex tube while the other end contained measured amounts of pristine $CoCl_2$ and $AlCl_3$ (the weight of $AlCl_3$ used was $\sim 10\%$ of that of $CoCl_2$). Before sealing the ampoule, it was evacuated and then partially filled with Cl_2 gas (at a pressure of ~ 300 Torr). The reaction ampoules thus prepared were placed inside a two-zone furnace in which the temperature of the host HOPG was kept at ~ 490 °C and the temperature of the chlorides a few degrees below 490 °C. The ampoules were kept inside the furnace for about 4 to 8 d. The details of the growth parameters for the samples used in this study are reported elsewhere.[17]

In our sample growth, we used $AlCl_3$ as a complexing halide[18] because no successful well-staged intercalation of HOPG with $CoCl_2$ by itself has yet been achieved. The role of $AlCl_3$ as a complexing halide has been discussed previously.[18] However, in contrast to the reports of Ref. 18 where no trace of $AlCl_3$ was observed in the intercalated graphite-$CoCl_2$ samples, our recent investigations using Auger spectroscopy and x-ray fluorescence[12,13] have revealed that significant amounts of $AlCl_3$ are present in our samples (see below). Recent characterization of the samples used in the present study by electron microscopy,[12,13] however, has shown that within the intercalate layers, the $CoCl_2$ forms rather large needle-shaped islands (about 100×500 Å^2). Of major significance is the observation that in the intercalate layers the $CoCl_2$ needles contain no $AlCl_3$, and likewise the $AlCl_3$ background contains no $CoCl_2$.[13] Thus the magnetic properties discussed here are appropriate to two-dimensional layers of magnetic ions.

The stage (number of contiguous graphite planes between the neighboring layers of $CoCl_2$) was determined using $(00l)$ x-ray diffractograms. The $K\alpha$ radiation of a molybdenum source and a Si(Li) detector were used. A single-channel analyzer was employed to provide discrimination of the incident x-ray energy, thus permitting the identification of small concentrations of admixed stages. The samples reported here all showed $(00l)$ diffractograms characteristic of single-stage samples.[17] The chemical formulas $C_{\xi n}X$, where X stands for $(CoCl_2)_{1-q}(AlCl_3)_q$, were determined from chemical analysis.[19] For each sample the weight percentages of the elements C, Al, Co, and Cl were determined, and using the stage determination by x rays, the parameters ξ and q in the above chemical formulas were found; the results are listed in Table I. To determine the values of q in Table I, we used only the measured weight percentages of Co and Al. As a check on the

TABLE I. Summary of the parameters in the chemical formula $C_{\xi n}X$, where X stands for $(CoCl_2)_{1-q}(AlCl_3)_q$, for the samples used in this study.

Stage n	ξ	q	Amt. Cl expected[a]	Amt. Cl measured[b]	wgt.$[X]$[c] / wgt.$[C_{\xi n}X]$	wgt.$[X]$[d] / wgt.$[C_{\xi n}X]$
2	7.93	0.63	2.66	2.63	0.412	0.413
4	7.07	0.68	2.68	2.29	0.281	0.284
5	7.04	0.73	2.73	2.86	0.245	0.248

[a]The amount of Cl expected is equal to $2(1-q)+3q$.
[b]Amount of Cl as measured by the chemical analysis.
[c]Deduced from the results of the chemical analysis (i.e., using the parameters ξ and q in this table).
[d]Deduced from our weight-uptake measurements.

consistency of the chemical analyses results, we compared the expected amount of Cl in a compound $C_{\xi n}(CoCl_2)_{1-q}(AlCl_3)_q$, which is equal to $[2(1-q)+3q]$, to the amount of Cl determined by the chemical analysis. These values are listed in the fourth and fifth columns of Table I and are in very good agreement.[20] Also, the last two columns of Table I contain values of weight $[X]$/weight $[C_{\xi n}X]$ deduced from the results of the chemical analysis, and our weight-uptake measurements. The excellent agreement (to within approximately 1%) between these values is another indication of the overall accuracy and consistency of the results of the chemical analysis. We estimate the accuracy of the parameters ξ and q in $C_{\xi n}(CoCl_2)_{1-q}(AlCl_3)_q$ to be approximately equal to $\pm 2\%$ for the samples reported in this study.

There have been very few measurements of heat capacity of small samples in high magnetic fields ($H > 10$ T). Such measurements are complicated because of the unavailability of small (approximately a few mg) thermometers with reliable accuracy in high magnetic fields. Recently Stewart *et al.*[21] successfully carried out heat-capacity measurements in fields as high as 18 T with the use of the relaxation time constant method.[22]

Our $C_p(T)$ measurements were done with the use of the weak-link heat-pulse method.[22,23] In this method, a "weak" thermal link connects the sample and the heat sink. When a small heat pulse of power P and duration Δt is applied to the sample, the temperature of the sample rises by an amount ΔT and then decays back to the sink temperature with a characteristic time constant τ. The total (sample plus addenda) heat capacity is given by[23]

$$C_{\rm tot} = (P\tau/\Delta T)(1-e^{-\Delta t/\tau}) , \quad (3)$$

which simply reduces to $C_{\rm tot} = P\,\Delta t/\Delta T$ for $\Delta t \ll \tau$. The time constant τ in Eq. (3) is also related to $C_{\rm tot}$ by

$$\tau = C_{\rm tot} R_t , \quad (4)$$

where R_t is the thermal impedance of the link. If R_t (which is a function of temperature) is known, then a measurement of τ will give $C_{\rm tot}$ (the time-constant method).[22] In our measurements we used Eq. (3) to determine $C_{\rm tot}$. We did not measure R_t in our laboratory directly; however, we note that if R_t is magnetic field independent, measurements of $C_{\rm tot}(T)$ using Eq. (3) in a given zero-field experiment permit us to determine R_t [in Eq. (4)] for the high-field experiment (which was carried out immediately after the zero-field experiment) as well. We are thus able to determine two nearly-independent values for the in-field $C_{\rm tot}$ [the relation between these two values is through τ, but for $\Delta t \ll \tau$, $C_{\rm tot}$ in Eq. (3) is nearly independent of τ]. We report here in-field heat-capacity data determined by Eq. (3), while the corresponding values found using Eq. (4) agreed to within 5% with these reported values. The disagreement is mainly due to our errors in measuring τ, which was noise limited.

Figure 1 shows the schematic setup for our heat-capacity measurements. This figure shows the sample chamber of our cryostat which is similar in design to the one used for our previously reported[24] high-field thermal-conductivity measurements and will be described in detail elsewhere.[17] The sample is suspended by fine nylon

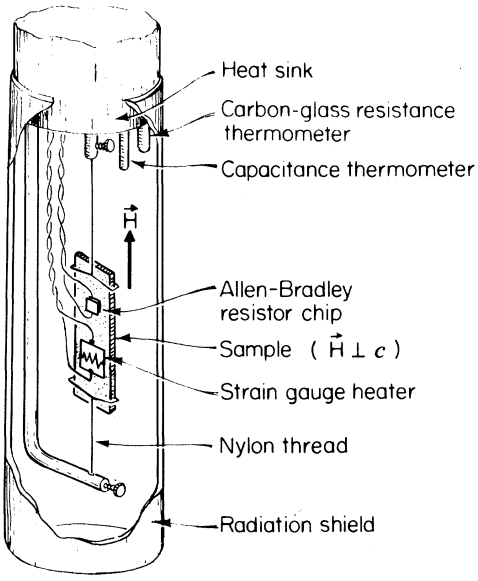

FIG. 1. Schematic representation of the experimental sample chamber for the heat-capacity measurements using the weak-link heat-pulse method. Magnetic field provided by a Bitter magnet is applied in the plane of the intercalate (perpendicular to the c axis of the sample).

threads in an isothermal copper can, evacuated to about 10^{-6} Torr (Fig. 1). A small chip (~ 1 mm^3) of a 100-Ω Allen-Bradley (AB) resistor and a small 110-Ω strain gauge heater were glued to the sample using very small amounts of diluted GE7031 varnish. Four pieces of an alloy wire (Au + 7% Cu, about 0.068 mm in diameter) were twisted in pairs and were used as the electrical as well as the thermal links between the sample and the sink. This alloy wire was used as the thermal link because it has a nearly field-independent thermal conductance ($\Delta R_t/R_t^0$ for this wire is smaller than 0.005 up to 14 T).[21,25]

The thermometers used in these measurements were especially chosen to address the problems in thermometry in high magnetic fields. A calibrated carbon-glass (CG) resistance thermometer served as the primary temperature sensor, and a capacitance thermometer (Fig. 1) was used to regulate temperature above 4.2 K. Below 4.2 K, the temperature was controlled by pumping on the helium bath and regulating the pressure. The temperature stability of the sink for the range $2<T<25$ K was better than $\sim 0.05\%$. The AB chip, which was used as a resistance thermometer to measure values of ΔT in Eq. (3), was calibrated against the CG thermometer at the beginning of each run.

For the in-field measurements, corrections had to be made for the magnetoresistance of the CG and the AB thermometers. The CG thermometers have been recently calibrated in fields up to 19 T by Sample *et al.*[26] For the AB resistor, we prepared a calibration table similar to that of Ref. 26 using the data of Neuringer *et al.*,[27] who studied the magnetoresistance of the AB resistors up to 14 T. With the use of these tables, our accuracy in measuring ΔT values (with the AB sensor) was about $\pm 3\%$ (and about $\pm 2\%$ for zero-field measurements). The errors in the ΔT measurements, which were noise limited, determine the errors in the heat-capacity values reported in this paper.

All resistance measurements (for the CG and AB sensors) in this study were made using a four-point probe DC method. An on-line computer was used for the acquisition and analysis of the data.

To check the accuracy of our heat-capacity measurements and also to evaluate the heat capacity of the addenda, we measured the heat capacity of an HOPG sample (572 mg) and then repeated the measurements, keeping the addenda fixed but cleaving the HOPG sample to a smaller size (372 mg). Since the total heat capacity can be written as the sum of the values due to the sample and the addenda, with the use of the above measurements we were able to find the heat capacity of the addenda as well as that of HOPG as a function of temperature (Fig. 2). The heat capacity of HOPG agreed with previously reported values[28] to better than 5% in the range $2<T<25$ K (see below). For the samples reported here, the addenda contribution to the heat capacity was less than $\sim 20\%$, and has been corrected for in the results presented in this paper. We also made in-field ($\vec{H}\perp\hat{c}$) measurements on HOPG (nonmagnetic material), and found no change in the heat capacity of HOPG with respect to the zero-field values (within $\pm 3\%$, which is the accuracy of our in-field measurements).

III. RESULTS AND ANALYSIS

In Fig. 2 the zero- and high-field C_p data for the $C_{\xi n}(CoCl_2)_{1-q}(AlCl_3)_q$ compounds of stages 2, 4, and 5 as well as C_p for HOPG are shown as a function of temperature on a log-log plot. With the use of previously adopted conventions,[28] the effective molar weight of a sample with the above chemical formula is given by

$$\frac{\xi n\, m(\mathrm{C})+(1-q)\, m(\mathrm{CoCl_2})+q\, m(\mathrm{AlCl_3})}{\xi n+3(1-q)+4q},$$

where $m(X)$ is the atomic (or molecular) weight of X. Figure 2 shows that $C_p(T)$ for HOPG follows a T^n dependence ($n=2.38$ as discussed below) in the temperature range $3<T<20$ K. The zero-field heat-capacity data, $C_p^0(T)$, for the intercalated samples show broad anomalies at $T\simeq 9$ K, while the heat capacities measured at $H^*=14$ T, namely $C_P^{H^*}(T)$, indicate a suppression of the zero-field anomaly and a downshift of the zero-field values over the

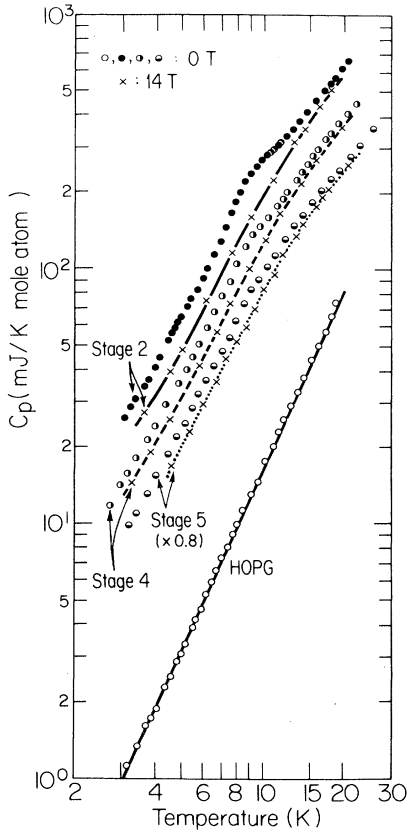

FIG. 2. Zero-field (C_p^0) and high-field ($C_p^{H^*}$; where $H^*=14$ T) heat capacities of the graphite-$CoCl_2$-$AlCl_3$ compounds (the data for the stage-5 compound have been reduced by a factor of 0.8 for clarity). The anomaly in the zero-field heat capacity (at $T\simeq 9$ K) is suppressed in the high-field data. The curves drawn through the high-field $C_p^{H^*}$ are polynomials (in temperature) fitted to the data points and are used to determine experimental $C_M(T)$ in Fig. 8. The heat capacity of HOPG (open circles) is also shown and is best represented by $C_p=0.0675\ T^{2.38}$ mJ/K$^{2.38}$ mole (the fitted solid line through the open circles).

entire temperature range $3 < T < 20$ K.

Figure 3 shows the magnetic field dependence of the percentage downshift of the heat capacity $[\Delta C_p(H) = C_p^0 - C_p^H]$ for the three intercalated samples for several indicated temperatures. This figure shows that ΔC_p at a given temperature nearly saturates at the highest fields, thus supporting our assumption that the spin-aligned paramagnetic state is well established at $H^* = 14$ T. Therefore, referring to Fig. 2 and using Eq. (2), we can write

$$C_E(T) + C_L(T) = C_p^{H^*}(T) , \tag{5}$$

$$C_M(T) = C_p^0(T) - C_p^{H^*}(T) , \tag{6}$$

where $H^* = 14$ T. We also measured the heat capacity of a stage-5 graphite-$AlCl_3$ sample at zero magnetic field. The $C_p(T)$ curve for this compound yielded an identical temperature dependence to the high-field data shown in Fig. 2 for the stage-5 graphite-$CoCl_2$-$AlCl_3$ compound [the $C_p(T)$ values agreed to better than 10% for the two samples]. Note that the $C_p^0(T)$ data for the stage-5 graphite-$CoCl_2$-$AlCl_3$ compound which has mostly $AlCl_3$ as the intercalant ($q = 0.73$; see Table I), apart from the magnetic part, is expected to be similar to a stage-5 graphite-$AlCl_3$ compound. Thus the above observation verifies that Eq. (5) is valid and that the magnetic contribution to $C_p^0(T)$ is almost entirely suppressed at the highest field $H^* = 14$ T.

In order to estimate the errors in $C_E(T) + C_L(T)$ and $C_M(T)$ in Eqs. (5) and (6) due to the incompleteness of the saturation of the curves shown in Fig. 3, we use the following extrapolation scheme. If we describe the field dependence of the shift in C_p shown in Fig. 3 by the empirical relation

$$\Delta C_p(H)/C_p^0 = AH^2/(1 + BH^2) , \tag{7}$$

then plots of $H^2/(\Delta C_p(H)/C_p^0)$ vs H^2 should be linear, and the inverse of the slope (A/B) is equal to the limiting high-field value for $\Delta C_p(H \to \infty)/C_p^0$. An example of such a plot is shown in Fig. 4 for the stage-2 graphite-$CoCl_2$-$AlCl_3$. The validity of the above empirical field dependence [Eq. (7)] is justified by the linear behavior of the data points shown in Fig. 4. [A function of the form

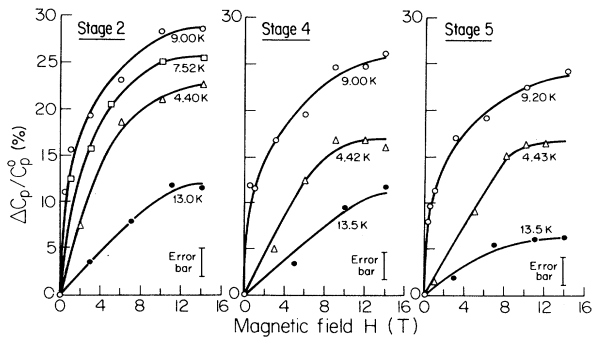

FIG. 3. Magnetic field dependence of the percentage downshift of the heat capacity $[\Delta C_p(H) = C_p^0 - C_p^H]$ for several indicated temperatures for graphite-$CoCl_2$-$AlCl_3$ compounds of stages $n = 2$, 4, and 5.

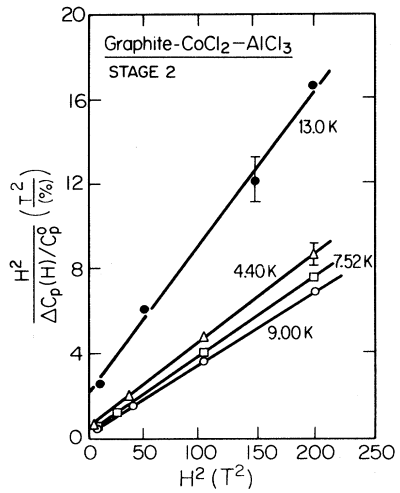

FIG. 4. Plots of $H^2/[\Delta C_p(H)/C_p^0]$ vs H^2 for the downshift of the heat-capacity data of the stage-2 graphite-$CoCl_2$-$AlCl_3$ sample given in Fig. 3. The saturation value of the downshift is given by the inverse slope of each line (see text).

$$\Delta C_p(H)/C_p^0 = AH/(1 + BH)$$

was also tried, but the fit to the data is not as good as that for Eq. (7).]

In Table II we compare $[\Delta C_p(H^* = 14\ \text{T})]/C_p^0$ to $[\Delta C_p(H \to \infty)]/C_p^0$ (which is equal to A/B) obtained from the inverse of the slopes of the plots, such as shown in Fig. 4, for compounds of different stages. Table II indicates that $C_E(T) + C_L(T)$ as determined by Eq. (5) is overestimated by approximately 2%, while the $C_M(T)$ determined by Eq. (5) is underestimated by approximately 3%.

Note in Fig. 3 that near the transition temperature (~ 9 K) the heat capacity drops sharply at low fields ($H < 1$ T), while it decreases less rapidly for $H > 1$ T. Such low-field anomalous behavior has also been reported in the magnetic susceptibility data for these compounds.[4,12,13] However, the field range where the rapid decrease of the peak susceptibility changes abruptly is much lower than 1 T.[4,12,13]

TABLE II. Comparison of the downshift in heat capacity $\Delta C_p(H^* = 14\ \text{T})/C_p^0$ with the saturation values $\Delta C_p(H \to \infty)/C_p^0$ obtained from the inverse slope (A/B) of plots such as shown in Fig. 4 for the graphite-$CoCl_2$-$AlCl_3$ compounds (see text).

Stage n	Temperature (K)	A/B (%)	$\Delta C_p(14\ \text{T})/C_p^0$ (%)
2	4.40	23.9	22.7
	7.52	26.7	25.6
	9.00	29.5	28.6
	13.0	13.7	11.6
4	4.42	18.4	16.0
	9.00	28.0	26.1
	13.5	15.7	11.8
5	4.43	18.5	16.5
	9.20	26.1	24.3
	13.5	7.3	6.4

Also, note in Fig. 3 that the magnitude of $\Delta C_p/C_p^0$ for a given temperature correlates with the amount of the magnetic material ($CoCl_2$) in the samples, i.e., $\Delta C_p/C_p^0$ is larger for lower-stage compounds. We note in Fig. 2 that $C_p^{H^*}(T)$ exhibits an approximate T^2 temperature dependence in the range $3<T<10$ K, while above ~ 10 K it deviates towards a lower power of temperature ($\sim T^{1.5}$). In the next section this temperature dependence of $C_p^{H^*}(T)$ is discussed in terms of a Debye model for the heat capacity of a two-dimensional lattice. The magnetic heat capacity $C_M(T)$ in Eq. (6) will also be discussed and compared to theoretical predictions based on the 2D XY model for magnetic ordering.[15]

IV. DISCUSSION

A. Electronic and lattice heat capacity

The electronic contribution to the heat capacity C_E for an interacting electron gas is generally written as $C_E=\gamma T$, where γ is determined by the electronic density of states at the Fermi level $N(E_F)$:

$$\gamma=\tfrac{1}{3}\pi^2 k_B^2(1+\lambda)N(E_F)\ , \tag{8}$$

where λ is the electron-phonon enhancement factor and has a value $0<\lambda<0.3$.[28] According to the Debye model, the lattice heat capacity C_L in three-dimensional solids usually shows a T^3 dependence at low temperatures. Application of the Debye model to a 2D lattice, however, results in a T^2 dependence for C_L (Ref. 17):

$$\begin{aligned} C_L &= 28.8Nk_B(T/\Theta_D)^2 \\ &= (2.39\times 10^5\ \text{mJ/K mole})(T/\Theta_D)^2\ , \end{aligned} \tag{9}$$

where N is Avogadro's number, k_B is Boltzmann's constant, and Θ_D is the Debye temperature.

1. Heat capacity of HOPG

First, we briefly discuss the heat-capacity results for HOPG (Fig. 2). The $C_p(T)$ data shown in Fig. 2 for HOPG are best represented by a function of the form $C_p(T)=\beta T^{2.38}$, where $\beta=0.0675\pm0.0010$ mJ/K$^{3.38}$ mole. This temperature dependence of C_p for HOPG is in very good agreement with previously reported results[28] which indicated that while the linear electronic contribution is very small, the lattice contribution C_L varies as T^3 only at the lowest temperatures (below ~ 10 K), tending towards a $T^{2.3}$ dependence above $T\simeq 10$ K. Our result is also in excellent agreement with previous measurements of $C_p(T)$ on synthetic graphite, which is reported to exhibit a $T^{2.38}$ dependence in the range 1–22 K (quoted in Ref. 29). This dependence of C_p on a power of T lower than 3 is attributed to the predominantly 2D phonon spectrum for HOPG.[28]

2. Electronic heat capacity of graphite-$CoCl_2$-$AlCl_3$ and the Shubnikov–de Haas measurements

For the intercalated compounds reported in this study, the electronic plus lattice contributions to C_p [i.e., $C_p^{H^*}(T)$ in Fig. 2 and Eq. (5)] in the range $3<T<10$ K can be best represented by $\gamma T+\beta T^2$. Values of γ and β determined from the least-squares fit of the above functional form to $C_p^{H^*}(T)$ in the range $3<T<10$ K are tabulated in Table III. Note that the values of γ are very small and are comparable to their inaccuracies, indicating that the electronic contribution to C_p is negligible compared to the lattice contribution in this temperature range. Such *small* values of γ are consistent with results of other heat-capacity measurements on acceptor GIC (Refs. 2, 5, and 30) where a T^2 dependence is observed for the C_E+C_L contribution. [Note that the small electronic contribution to the heat capacity observed for the acceptor GIC is entirely due to graphite electrons and is thus qualitatively different from the large electronic contribution to C_p reported for stage-1 donor GIC at low temperatures ($1.5<T<4$ K).[28,31,32]] These small-γ values are also consistent with results of our Fermi-surface (FS) studies on graphite-$CoCl_2$-$AlCl_3$, which are performed on compounds of stages 3 and 4 with the use of the Shubnikov–de Haas (SdH) technique and are presented below.

We measured the FS extremal cross sections perpendicular to the c axis by studying the oscillatory behavior of the in-plane magnetoresistance (ρ_{osc}) of these compounds while the magnetic field H which was applied parallel to the c axis was swept up to 14 T. The Fourier transform (power spectrum) of ρ_{osc} vs $1/H$ yields the frequencies ν_i of the SdH oscillations, which are directly related to the FS extremal cross sections.[33,34] Such a Fourier power spectrum is shown in Fig. 5 for a stage-3 graphite-$CoCl_2$-$AlCl_3$ sample. The values of observed ν_i are listed in Table IV. To account for the observed FS cross sections, we use the rigid-band (dilute-limit) model[35] and c-axis zone folding.[34,36] In this model the Slonczewski-Weiss-McClure (SWMcC) model[36] for the π bands of graphite is used, and the effect of intercalation for a stage-n acceptor compound is assumed to be a transfer of charge from the n graphite layers to the intercalate layer, thus lowering the Fermi level E_F relative to $E_F^0=-0.024$ eV for pristine graphite, where the zero of energy is taken at the H-point band extremum. The position of E_F is determined by the requirement that the largest predicted SdH frequency (the FS cross section at the K point) coincides with the largest observed frequency. Next, the effect of superlattice periodicity due to staging is considered, and zone folding along the k_z direction is introduced to find the extremal cross sections of the FS in the folded Brillouin zone.[34,36] The result of such an analysis is shown in Fig. 5 by five arrows, which indicate the positions of the predicted SdH

TABLE III. Electronic and lattice heat-capacity parameters for the graphite-$CoCl_2$-$AlCl_3$ compounds, obtained by fitting a function of the form $\gamma T+\beta_n T^2$ to the high-field C_p data in the temperature range $3<T<10$ K. The Debye temperatures Θ_D are obtained using Eq. (9).

Stage n	γ mJ/K^2 mole atoms	β_n mJ/K^3 mole atoms	Θ_D (K)
2	0.06±0.05	1.71±0.06	380±7
4	0.08±0.05	1.06±0.05	480±9
5	0.04±0.05	0.83±0.04	540±12

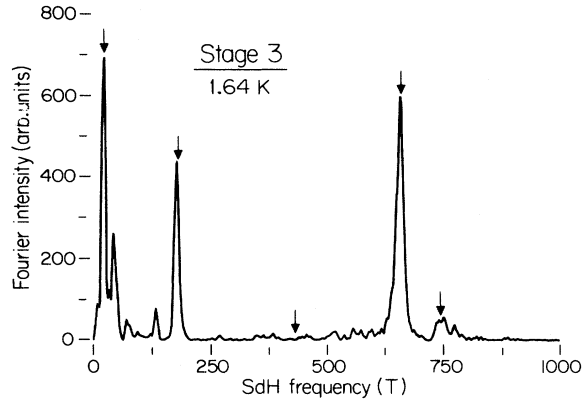

FIG. 5. Fourier power spectrum for a stage-3 graphite-$CoCl_2$-$AlCl_3$ sample at $T=1.64$ K. The positions of the peaks correspond to the Shubnikov–de Haas (SdH) frequencies which are in turn related to the Fermi-surface cross sections (perpendicular to H which is applied parallel to the c axis of the sample). The lowest SdH frequency (at 22 T) has harmonics at 43, 65, and 89 T. The arrows indicate the positions of the calculated SdH frequencies (see Table IV).

frequencies, and in Table IV which lists the frequency values. The E_F value used in the analysis is -0.675 eV, and the carrier concentration is $p=1.0\times10^{21}$ cm^{-3}, which is similar to values reported for other acceptor GIC.[36] This carrier concentration results in a fractional charge transfer per intercalant (f_X) equal to 0.37, which is typical for acceptor GIC.[36] Examination of Fig. 5 and Table IV shows that, considering the simplicity of the model used, the agreement between the experimental and theoretical ν_i is very good.

We also measured the temperature dependence of the amplitudes of the SdH oscillations. We were able to detect oscillations in the magnetoresistance up to ~77 K which is the highest temperature at which SdH oscillations have been reported for GIC.[37] The temperature-dependent part of the amplitude of the SdH oscillations A can be written as[33,38]

$$A=\frac{\alpha}{\sinh(\alpha)}\ , \tag{10}$$

where α is equal to $14.7(m^*/m_0)(T/H_0)$ in SI units (m^* is the cyclotron effective mass and H_0 is the field at which the amplitude is measured). In Fig. 6 we show plots of $\ln(A/T)$ vs T for the 176- and 656-T SdH frequencies. The data are very well fitted by a function of the form given by Eq. (10) (the solid curves in Fig. 6), and provide the (cyclotron) effective masses which are listed in Table IV. Note that for $\alpha>3$, Eq. (10) predicts an approximately linear behavior for $\ln(A/T)$ vs T, which is in fact observed in Fig. 6 for $T>9$ K. In Table IV, the m^*/m_0 values measured for the different frequencies are compared to the cyclotron effective masses defined by

$$m^*=\frac{\hbar^2}{2\pi}\frac{dS}{dE}\bigg|_{E=E_F}\ , \tag{11}$$

where S is the FS cross section perpendicular to the direction of $\vec{H}$. The calculated m^*/m_0 listed in Table IV are predictions of the rigid-band model (and zone folding) for the different calculated cross sections indicated in the same table. There is again very good agreement between the measured and calculated effective masses, further verifying the graphitic nature of the bands in this compound.

Returning to the estimation of the electronic contribution to the heat capacity, we use $E_F=-0.675$ eV to find $N(E_F)$ for this stage-3 compound. Using $\lambda=0$ in Eq. (8), we then obtain $\gamma\cong0.15$ mJ/K^2 mole atoms, which is consistent within the experimental error values determined from the heat-capacity measurements (see Table III).

TABLE IV. Summary of the observed and calculated Shubnikov–de Haas frequencies ν_i (in units of T) and the cyclotron effective masses m^*/m_0 for a stage-3 graphite-$CoCl_2$-$AlCl_3$ compound. The Fermi level used in the analysis is $E_F=-0.675$ eV.

Observed		Calculated	
m^*/m_0	$\nu(T)$	$\nu(T)$	m^*/m_0
	749	745	0.29
0.22 ±0.02	656	660	0.26
		433	0.20
0.11 ±0.01	176	181	0.13
	132		
0.032±0.01	22	23	0.083

3. *Lattice heat capacity of graphite-$CoCl_2$-$AlCl_3$*

The lattice contribution to the heat capacity of the intercalation compounds [$C_L(T)=\beta T^2$] can be understood in terms of a Debye model for a 2D lattice [Eq. (9)]. Using Eq. (9) we have determined values for Θ_D, which are listed in Table III. These values for Θ_D are of the order of

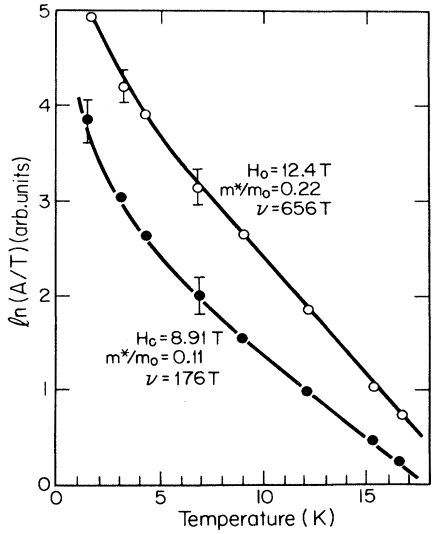

FIG. 6. Plot of $\ln(A/T)$ vs T where A is the amplitude of SdH oscillations and T is the temperature in K for the indicated SdH frequencies ν_i for the stage-3 graphite-$CoCl_2$-$AlCl_3$. In each case the cyclotron effective mass values are determined from least-squares fitting the solid curves, which have the functional form given by Eq. (10), to the data.

Θ_D for HOPG ($\simeq$430 K) and are comparable to the values reported for other donor GIC's.[28] Also, note in Fig. 2 that the $C_L(T)$ [which is approximately equal to $C_p^{H^*}(T)$, since $C_E(T)$ is small] data show deviations from a T^2 dependence towards a less rapid temperature dependence above $\sim$10 K; we note that 10 K corresponds to about $\Theta_D/50$, above which deviations are expected from the Debye model.

In Table III we note that the smaller values of β correspond to compounds of higher stage (Fig. 7 shows the stage dependence of β).[39] A similar stage dependence of the lattice contribution to C_p has been recently reported for the Rb-GIC system.[31] The lattice heat capacity of the graphite-bromine compounds is also reported to increase as the bromine concentration increases.[40] These observations indicate that the dependence of β on stage must be related to those lattice vibrations in which the intercalate atoms or molecules participate.[31] We may express the lattice heat-capacity coefficient β_n for a stage-n compound $C_{\xi_n n}(CoCl_2)_{1-q}(AlCl_3)_q$ as[31]

$$\beta_n = \frac{[3(1-q)+4q+2\xi_n]\beta_{Cb}+(n-2)\xi_n\beta_{Ci}}{3(1-q)+4q+n\xi_n} , \quad (12)$$

where β_{Cb} and β_{Ci} are the heat-capacity coefficients for the graphite bounding and interior layers. First, note that if we calculate

$$\beta'_n=[3(1-q)+4q+n\xi_n]\beta_n$$

using the data of Tables I and III, we find $\beta'_n=33.3$, 33.9, and 32.4 mJ/K^3 for $n=2$, 4, and 5, respectively, meaning that β'_n does not depend on stage (within the experimental accuracy; see β_n values in Table III). We thus infer that the contribution from the β_{Ci} term in Eq. (12) must be small. This is not surprising since β for HOPG, which we expect to be close to β_{Ci}, is only $\sim$0.094 mJ/K^3 mole,[39] while if we use the data for the stage-2 ($n=2$) compound in Eq. (12) we obtain $\beta_{Cb}=1.71\pm0.06$ mJ/K^3 mole atom. We therefore use $\beta_{Cb}=1.71$ mJ/K^3 mole atom and $\beta_{Ci}=0.094$ mJ/K^3 mole atom in Eq. (12) and calculate $\beta_4=1.00$ mJ/K^3 mole atom and $\beta_5=0.86$ mJ/K^3 mole atom in very good agreement with the values in Table III. [The dashed curve in Fig. 7 is a representation of Eq. (12) using the above values for β_{Cb} and β_{Ci}.] The lattice heat capacity for the graphite-$CoCl_2$-$AlCl_3$ is thus seen to be dominated by the contribution from the bounding layers ($\beta_{Cb} \gg \beta_{Ci}$) and is well represented by Eq. (12) in agreement with the observed behavior for Rb-GIC.[31]

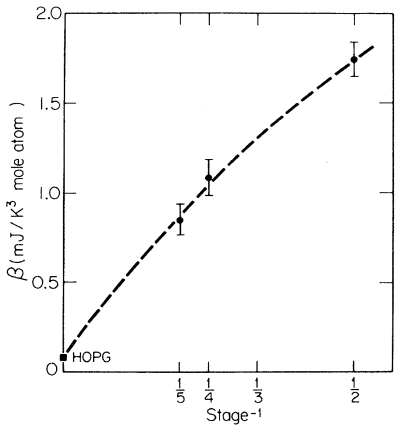

FIG. 7. Trend of the lattice heat-capacity coefficient β as a function of reciprocal stage for the graphite-$CoCl_2$-$AlCl_3$ compounds and for HOPG (stage ∞) (Ref. 39).

B. Magnetic heat capacity

In Fig. 8 the magnetic heat capacities C_M determined using Eq. (6) are plotted for the compounds reported in this study. The C_M curves shown in Fig. 8 all show broad peaks at $T^{max}=9.1\pm0.4$ K, in agreement with previous reports of the heat capacity for graphite-$CoCl_2$ by Karimov,[2] who finds $T^{max}=9.08$ K for a stage-2 compound. In Fig. 8 note that the size of the error bar is large [due to the subtraction of two large numbers; see Eq. (6)]. The errors are especially large in the temperature range $T>9$ K and for the higher-stage compounds because, as Fig. 2 shows, the C_M contribution to the heat capacity is only $\sim$10% of C_p^0 in this range. It is seen in Fig. 8, however, that the peaks in $C_M(T)$ for stages 4 and 5 are broader than that for the stage-2 compound. This is consistent with magnetic susceptibility measurements on the same compounds[6,12,13] which also indicate broader susceptibility peaks for higher stage samples.

The entropy S associated with the phase transition can be found from the experimental C_M data shown in Fig. 8 by

$$S=\int (C_M/T)dT . \quad (13)$$

The entropies determined using Eq. (13) for the three compounds are listed in Table V. These entropies are about 63% of the (maximum) theoretically expected value S' equal to $R\ln(2J+1)=5.76$ J/K mole $CoCl_2$, where R is the gas constant equal to 8.32 J/K and $J=\frac{1}{2}$ for $CoCl_2$.[10] These values of S/S' are consistent with values reported previously for graphite-$FeCl_3$ and graphite-$NiCl_2$ compounds ($0.61\leq S/S'\leq 0.73$),[5] and suggest that there may be additional magnetic ordering at temperatures outside the range studied here.

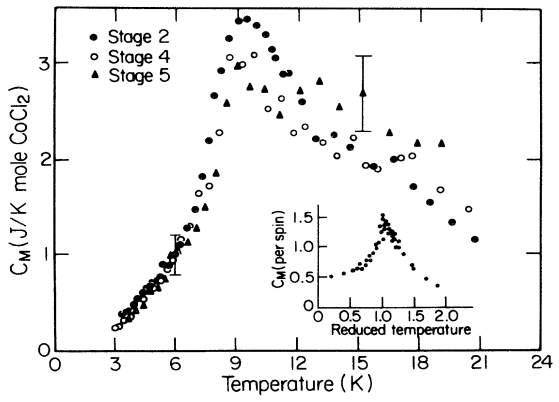

FIG. 8. Magnetic heat capacity $C_M(T)$ for the graphite-$CoCl_2$-$AlCl_3$ compounds determined by using Eq. (6) and the data shown in Fig. 2. The theoretical $C_M(T)$ curve shown in the inset is the reported result of a Monte Carlo calculation of heat capacity based on the XY model (Ref. 15).

To compare our experimental $C_M(T)$ curves with predictions of the XY model, we show in the inset in Fig. 8 the results of a Monte Carlo (MC) calculation[15] of $C_M(T)$ based on the XY model. The scatter of points in this theoretical C_M curve is due to the fact that computer simulation was used to perform the MC calculations.[15] Considering the experimental and theoretical uncertainties, the general shape of the C_M curves shown in Fig. 8, especially the *broadness* of the peaks, are in fair agreement. The broad peaks observed in Fig. 8 are in direct contrast to the very sharp heat-capacity anomalies expected and observed for other types of magnetic phase transitions (such as the antiferromagnetic phase transition observed in pristine $CoCl_2$).[10] The maximum values of the magnetic heat capacity observed for the three compounds are listed in Table V under C_M^{max}. These values of C_M^{max} are only about 30% of the maximum C_M predicted by MC calculations (i.e., $C_M^{max} \simeq 1.3R \simeq 12$ J/K mole spin; see the inset to Fig. 8). This discrepancy may again be due to the incompleteness of the magnetic ordering.

The small value of our experimental C_M^{max} may also be due to the fact that the magnetic interactions in our compounds are very likely not of a pure XY type. In fact, the magnetic Hamiltonian for pristine $CoCl_2$ [Eq. (1)] indicates an XY-type anisotropy of $J_A/J = 0.56$. In a recent MC simulation of the 2D classical Heisenberg model with 1% "easy-plane" XY anistropy, Kawabata and Bishop[41] have calculated the specific heat. They find a very broad anomaly for C_M at the reduced temperature of $k_B T/J \cong \frac{2}{3}$. The maximum value of this C_M "peak" is about 0.4, which is approximately $\frac{1}{3}$ of C_M^{max} for the MC calculations for the pure XY model as shown in the inset to Fig. 8. It is possible, then, that the small value of the experimental C_M^{max} for our samples may be due to the deviation of our physical system from the ideal XY model.

It is seen in Fig. 8, however, that as $T \to 0$ the MC calculation of C_M approaches $\frac{1}{2}R$ (per spin) while the experimental C_M approaches zero. This is because in the MC calculations no in-plane anisotropy (no in-plane preferred direction due to crystalline fields) is assumed, and thus C_M approaches $\frac{1}{2}R$, which is the expected behavior for magnons. In our compounds it is likely that the presence of a sixfold in-plane field quenches the magnons at $T \to 0$. Even in the absence of a sixfold field, since magnons are present at both zero and high fields, our experimental $C_M(T)$ [determined using Eq. (6)] will not show any magnon contribution. Note also in Fig. 8 that if Eq. (13) is used to calculate the entropy for the Monte Carlo C_M, we find $S \to \infty$ (since C_M is nonzero at $T \to 0$). This is indeed expected insofar as the XY model is a classical model. Therefore, it is evident that a more instructive comparison between the theoretical C_M and S and our experimental values can only be made if the effects of the symmetry-breaking field are incorporated into the theory. Such a calculation is presently underway.[42]

The MC calculations[15] for C_M report that the critical temperature T_c for the phase transition is about 15% below the temperature at which C_M attains its peak (T^{max}). Matching the peaks of the experimental and the Monte Carlo $C_M(T)$ curves, we find that $T_c = 7.9 \pm 0.2$ K for the stage-2 compound shown in Fig. 8. This determination of T_c is in good agreement with $T_c = 8.3$ K deduced from the susceptibility studies on the same compound.[6,12,13]

Finally, in Fig. 8 we note that the peaks in $C_M(T)$ for the higher-stage compounds have a smaller maximum and are also broader (see Table V for a listing of C_M^{max} values for the three compounds). A possible explanation for the difference in C_M^{max} values could be given in terms of the size of the spin islands in these compounds. The MC calculations for C_M shown in the inset of Fig. 8 were performed for square spin lattices of size 900, 3600, and 10 000 spins, and no significant effects due to the size of the lattice were observed.[15] More recent calculations of C_M (based on a 2D XY model) have been made for spin lattices of smaller size (25, 49, 100, 225, 625, and 1600 spins).[43] The $C_M(T)$ determined by these calculations agreed well with those of Ref. 15 for the lattices of size larger than 225. However, for the smaller lattices a systematic drop in the maximum value of C_M was reported (up to 30% of the maximum C_M^{max} of the largest lattices). The C_M peaks were also considerably broader for the smaller lattices.

Therefore, it is possible to explain the stage dependence of the shape of the C_M data shown in Fig. 8 if we assume that the intercalant ($CoCl_2$) islands are small (~ 100 spins) and that the island size decreases for compounds of higher stage. We note, however, that in our system an island of 100 spins occupies an area of about 20×30 Å^2, which is an order of magnitude smaller than the $CoCl_2$ island size observed in these compounds using electron microscopy.[12,13] Also, an examination of the data in Table I reveals that the relative amounts of $CoCl_2$ and $AlCl_3$ in these samples decrease with increasing stage [$(1-q)/q$ is equal to 0.59, 0.47, and 0.37 for stages $n = 2$, 4, and 5, respectively]. This observation supports the idea that $CoCl_2$ islands may be smaller in higher-stage compounds. To justify such an assumption about the intercalate island size, however, more direct and careful investigations regarding the structure of these materials is needed.

TABLE V. Magnetic heat-capacity parameters for the graphite-$CoCl_2$-$AlCl_3$ compounds.

Stage n	T^{max}[a] (K)	C_M^{max} (J/K mole $CoCl_2$)	S (J/K mole $CoCl_2$)	S/S'[b]
2	9.1±0.2	3.6±0.4	3.6±0.7	0.62±0.13
4	9.1±0.4	3.2±0.4	3.4±0.6	0.60±0.12
5	9.0±0.6	3.1±0.4	3.9±0.8	0.68±0.14

[a] T^{max} is the temperature at which C_M attains its peak (C_M^{max}).

[b] $S' = R \ln(2J+1) = 5.76$ J/K mole $CoCl_2$, where J is assumed to be $\frac{1}{2}$ for $CoCl_2$ (see Ref. 10).

V. CONCLUSIONS

This work shows that high magnetic fields can be used to separate the magnetic contribution to the heat capacity from the lattice and electronic contributions for the graphite-$CoCl_2$-$AlCl_3$ compounds. Compared to the method of corresponding states, our method has the great advantage that the separation can be done using the same physical sample. In this work we also report the first systematic study of the different contributions to the heat capacity of a magnetic GIC as a function of stage. The lattice contribution exhibits a T^2 temperature dependence characteristic of a two-dimensional phonon spectrum, while the magnetic contribution C_M is qualitatively consistent with the results of the MC calculations based on the 2D XY model. Below T_c, the behavior of the experimental C_M is qualitatively different from the MC results. This discrepancy is attributed to the presence of an in-plane symmetry-breaking field in our compounds.

ACKNOWLEDGMENTS

The authors wish to thank Dr. L. Rubin, Dr. B. Brandt, and the staff at the Francis Bitter National Magnet Laboratory for technical assistance and advice. We thank M. Kardar, M. Elahy, Dr. S. Flandrois, and Dr. G. R. Stewart for useful suggestions. The HOPG material was kindly provided by Dr. A. W. Moore of the Union Carbide Co. We acknowledge the U.S. Air Force Office for Scientific Research Contract No. F49620-83-C-0011 for support of this work.

---

*Present address: Department of Physics and Astronomy, University of Maryland, College Park, MD 20910.

[1]A. V. Zvarykina, Yu. S. Karimov, M. E. Vol'pin, and Y. N. Novikov, Fiz. Tverd. Tela (Leningrad) 13, 28 (1971) [Sov. Phys.—Solid State 13, 21 (1971); Yu. S. Karimov, A. V. Zvarykina, and Yu. N. Novikov, *ibid.* 13, 2836 (1971) [13, 2388 (1971); Yu. S. Karimov, M. E. Vol'pin, and Yu. N. Novikov, Zh. Eksp. Teor. Fiz. Pis'ma Red. 14, 271 (1971) [JETP Lett. 14, 142 (1971)]; Yu. S. Karimov, *ibid.* 15, 332 (1972) [15, 235 (1972)]; Zh. Eksp. Teor. Fiz. 66, 1121 (1974) [Sov. Phys.—JETP 39, 547 (1974)]; Yu. S. Karimov and Yu. N. Novikov, Zh. Eksp. Teor. Fiz. Pis'ma Red. 19, 268 (1974) [JETP Lett. 19, 159 (1974)].

[2]Yu. S. Karimov, Zh. Eksp. Teor. Fiz. 68, 1539 (1976) [Sov. Phys.—JETP 41, 772 (1976)].

[3]M. Suzuki and H. Ikeda, J. Phys. C 14, L923 (1981).

[4]M. Elahy, C. Nicolini, G. Dresselhaus, and G. O. Zimmerman, Solid State Commun. 14, 289 (1982).

[5]D. G. Onn, M. G. Alexander, J. J. Ritsko, and S. Flandrois, J. Appl. Phys. 53, 2751 (1982).

[6]M. Elahy and G. Dresselhaus, in *Intercalated Graphite,* edited by M. S. Dresselhaus, G. Dresselhaus, J. E. Fischer, and M. Moran (Elsevier North-Holland, New York, 1983), p. 207.

[7]M. Shayegan, L. Salamanca-Riba, J. Heremans, G. Dresselhaus, and J.-P. Issi, *Intercalated Graphite,* Ref. 6, p. 213.

[8]J. M. Kosterlitz and D. J. Thouless, J. Phys. C 6, 1181 (1973); J. M. Kosterlitz, *ibid.* 7, 1046 (1974).

[9]J. V. José, L. P. Kadanoff, S. Kirkpatrick, and D. R. Nelson, Phys. Rev. B 16, 1217 (1977).

[10]R. C. Chisholm and J. W. Stout, J. Chem. Phys. 36, 972 (1962).

[11]M. T. Hutchings, J. Phys. C 6, 3143 (1973).

[12]M. Elahy, Ph.D. thesis, Massachussets Institute of Technology, 1983 (unpublished).

[13]M. Elahy, M. Shayegan, K. Y. Szeto, and G. Dresselhaus, in Proceedings of the Third International Conference on Graphite Intercalation Compounds, Pont à Mousson, France, 1983 [Synth. Met. (in press)].

[14]J. W. Stout and E. Catalano, J. Chem. Phys. 23, 2013 (1955).

[15]J. Tobochnik and G. V. Chester, Phys. Rev. B 20, 3761 (1979).

[16]A. Hérold, in *Physics and Chemistry of Materials with Layered Structures,* edited by F. Lévy (Reidel, Dordrecht, Holland, 1979), Vol. 6, p. 323.

[17]M. Shayegan, Ph.D. thesis, Massachusetts Institute of Technology, 1983 (unpublished).

[18]E. Stumpp, Mater. Sci. Eng. 31, 53 (1977).

[19]The chemical analyses were done by the Schwarzkopf Microanalytical Laboratory, Inc., Woodside, NY. The following methods were used in these analyses for determination of the amounts of the elements present: combustion of part of the sample and measurement of CO_2 gas for C, atomic absorption for Co and Al, reaction with Ag^+ and measurement of precipitated AgCl for Cl.

[20]The chemical analysis results show that the stage-4 sample is approximately 15% deficient in Cl (compare columns four and five of Table I). However, when the composition $C_{\xi n}(CoCl_2)_{1-q}(AlCl_3)_q$ is used (i.e., no deficiency in Cl is assumed) to find wgt.$[X]$/wgt.$[C_{\xi n}X]$, the agreement with the weight-uptake measurements is excellent (see last two columns of Table I). On the other hand, if we assume the deficiency in Cl is correct, we obtain wgt.[Al + Co + Cl]/wgt.[C + Al + Co + Cl] = 0.258 which is approximately 9% smaller than the weight-uptake value (0.284). We thus believe that the deficiency in Cl may be largely due to errors in the chemical analysis. Note, in any case, that an error of this magnitude in the amount of Cl present in the sample will not affect the accuracy of the magnetic contribution to C_p, and will only very slightly ($\lesssim 2\%$) increase the value of the lattice contribution β (see Sec. III) for this compound.

[21]G. R. Stewart, B. Cort, and G. W. Webb, Phys. Rev. B 24, 3841 (1981).

[22]R. Bachmann, F. J. DiSalvo, T. H. Geballe, R. L. Greene, R. E. Howard, C. N. King, H. C. Kirsch, K. N. Lee, R. E. Schwall, H.-U. Thomas, and R. B. Zubeck, Rev. Sci. Instrum. 43, 205 (1972).

[23]R. L. Fagaly and R. G. Bohn, Rev. Sci. Instrum. 48, 1502 (1977).

[24]J. Heremans, M. Shayegan, M. S. Dresselhaus, and J.-P. Issi, Phys. Rev. B 26, 3338 (1982).

[25]B. L. Brandt and G. R. Stewart (private communication).

[26]H. Sample, B. L. Brandt, and L. Rubin, Rev. Sci. Instrum. 53, 1129 (1982).

[27]L. J. Neuringer and Y. Shapira, Rev. Sci. Instrum. 40, 1314 (1969). Figure 4 of this reference was digitized and used to make the calibration table.

[28]M. G. Alexander, D. P. Goshorn, and D. G. Onn, Phys. Rev. B 22, 4534 (1980).

[29]B. T. Kelly, *Physics of Graphite* (Applied Science, London, 1981), p. 182.

[30]D. G. Onn, L. Q. Wang, Y. Obi, G. Holley, and P. C. Eklund, Bull. Am. Phys. Soc. 27, 405 (1982).
[31]M. Suganuma. T. Kondow, and U. Mizutani, Phys. Rev. B 23, 706 (1981).
[32]U. Mizutani, T. Kondow, and T. B. Massalski, Phys. Rev. B 17, 3165 (1978).
[33]G. Landwehr, *Physics of Solids in Intense Magnetic Fields,* edited by E. D. Haidemenakis (Plenum, New York, 1969), p. 415.
[34]The FS of many GIC has been recently measured using the magneto-oscillatory techniques. See M. Shayegan, M. S. Dresselhaus, and G. Dresselhaus, Phys. Rev. B 25, 4157 (1982) for some recent results on donor-GIC as well as for references for other GIC.
[35]M. S. Dresselhaus, G. Dresselhaus, and J. E. Fischer, Phys. Rev. B 15, 3180 (1977).
[36]M. S. Dresselhaus and G. Dresselhaus, Adv. Phys. 30, 139 (1981); see pp. 213—215.
[37]At the highest temperatures (>40 K) we could observe oscillations only for the smallest FS cross section ($\nu=22$ T) with a signal-to-noise ratio of about 3:1.
[38]D. Shoenberg, J. Magn. Magn. Mater. 11, 216 (1979).
[39]The β value shown in Fig. 7 for HOPG is from the curve $\beta T^{2.38}$ (see Fig. 2) and is equal to 0.0675 mJ/K$^{2.38}$ mole. The value of β found by fitting βT^2 to the data, however, is also small (about 0.09 mJ/K^3 mole).
[40]U. Mizutani, M. Suganuma, and T. Kondow, Solid State Commun. 43, 303 (1982).
[41]C. Kawabata and A. R. Bishop, Solid State Commun. 42, 595 (1982).
[42]K. Y. Szeto (private communication).
[43]J. E. Van Himbergen and S. Chakravarty, Phys. Rev. B 23, 359 (1981).